 DOI: 10.1002/masy.201100069

Micellization and Structure of MOPEO-*b*-PCL Copolymers and Their Application as Nanocontainers for Drugs

Sofia Partsevskaya,[*1] *Tatyana Zheltonozhskaya,*[1] *Yuriy Gomza,*[2] *Valeriy Klepko*[2]

Summary: Diblock copolymers (DBCs) of MOPEO-*b*-PCL containing biocompatible and biodegradable components: hydrophilic methoxypoly-(ethylene oxide) ($M_n = 2.5$ kDa = const) and hydrophobic poly(ε-caprolactone) of a variable chain length ($M_n = 2.8 \div 24.3$ kDa) were synthesized by an anionic ring-opening block copolymerization. Their chemical and microphase structure were characterized using FTIR, NMR, DSC and WAXS. Self-assembly of pure DBCs and those at the presence of a model drug prednisolon (PS) in dioxane/aqueous solutions was studied using visible spectroscopy and static light scattering. Increasing in the micellar stability at the PCL block lengthening and PS addition was revealed. The drug binding by DBC micelles due to hydrogen bonds and hydrophobic interactions was confirmed by FTIR.

Keywords: block copolymers; micelles; prednisolon; self-assembly; structure

Introduction

In recent years, the solution of a problem, concerned with effective drug delivery using nanoscaled carriers, receive special attention not only in medicine, but also in biochemistry and polymeric science. Treatment of tuberculosis, inflammatory diseases and, especially, cancer need new strategies, which can improve the efficacy and security of the therapy. Various drug carriers, such as solid lipid nanoparticles, macromolecular prodrugs, nanoparticles made of biodegradable natural and synthetic polymers, microcapsules, liposomes, naturally existing proteins (e.g. transferrin) and polymer micelles are currently under development.[1–5]

The macromolecular drug carrier should be able to minimize drug degradation and loss upon administration, prevent harmful side effects, and increase drug bioavailability and the fraction of the drug accumulated in the pathological area. For this purpose the therapeutic systems, based on amphiphilic biocompatible and biodegradable block copolymer micelles, have numerous advantages. The small size of the micelles and their surface characteristics provide prolonged circulation in the blood, high physiologically stability in biological environment, the ability of passive drug targeting and accumulating in various pathological sites *via* EPR-effect (the enhanced permeability and retention). The active drug targeting – the ability to specifically recognize and bind target tissues or cells – is also possible *via* the surface-attached specific stimuli-responsive ligands. The micelle carriers possess high loading capacity; they preserve the drug activity until it reaches the target site and even ensure control release in the site of action. Furthermore, such carriers are nontoxic, don't accumulate in the body and can be used for various routes of administration including oral, intravenous, nasal etc.[6–9]

Reasoning from the premises, we dedicated the present work to the studying of micellar systems obtained by the self-

[1] Department of Macromolecular Chemistry, Faculty of Chemistry, Kiev National Taras Shevchenko University, 64 Vladimirskaya St., 01033 Kiev, Ukraine
Fax: +380442393100;
E-mail: partsevskaya@ukr.net
[2] Institute for Macromolecular Chemistry, National Academy of Sciences of Ukraine, 48 Kharkovskoye Shosse, 02160 Kiev, Ukraine

assembling of amphiphilic block copolymers containing immiscible methoxypoly(ethylene oxide) (MOPEO) and poly(ε-caprolactone) (PCL). These components were chosen because of their nontoxic nature and inability to promote the generation of harmful substances within the body. The biocompatibility and resorbability of synthetic aliphatic polyester PCL and biomedical features of PEO are well known.[10,11] Moreover, coating nanoparticles with the poly(ethylene glycol) (PEG-coating) sterically hinders the interactions of blood components with their surface and reduces the binding of plasma proteins with PEG-coated nanoperticles.[12,13]

The self-assembling of amphiphilic block copolymers in selective solvents generally results in nanosized block copolymer micelles. The hydrophobic blocks tend to form the inner ''core'', which can act as an incorporation medium for various hydrophobic drugs, and the hydrophilic blocks form the outer ''shell'' or ''corona'', which (e.g. in the case of PEO blocks) is able to prevent uptake by the reticuloendothelial system, thus disallowing preliminary elimination of the micelles from the bloodstream.[14,15,16] Such micellar systems are known to enable up to several thousand times greater amounts of incorporated drugs to be administered in aqueous medium and increase a drug stability.[17] The micelles of the block copolymers are capable of internalizing into living cells by means of an endocytotic pathway. Also, some studies with the method of fluorescence labeling shown, that such micelles are suitable for the multiple cytoplasmic targeting.[17,18,19]

The size and morphology of the micelles, the nature and concentration of the dissolved drug, the loading efficiency of the micellar carrier, the way of drug incorporation into the micelle ''core'' (chemical attachment or physical encapsulation), and, finally, the method of preparation of the delivery system – all these factors significantly influence the drug loading.[20] Despite the living scientific interest to such block copolymer micellar nanocarriers,[4,18] many aspects of their micellization, structure and interaction with different compounds were studied insufficiently. Therefore, in the present study we try to cover some questions about a bulk structure and self-assembling processes of MOPEO-*b*-PCL copolymers, and also about the possibility and nature of entrapment of a model drug (synthetic hormone) prednisolon by these block copolymer micelles.

Experimental Part

In the syntheses of MOPEO-*b*-PCL copolymers the sample of methoxypoly(ethylene glycol) (MOPEG) with $M_v = 2.0$ kDa from ''Fluka'' (USA), ε-caprolactone (CL) from ''Sigma-Aldrich'' (USA) and stannous octoat from ''Acros Organics'' (USA) were used. The commercial crystalline prednisolon (PS) from ''Sigma Aldrich'' (USA) was used as a model drug.

Syntheses of the MOPEO-*b*-PCL diblock copolymers (DBCs) were carried out according to the total methodology by Bogdanov and co-workers[21] by an anionic ring-opening block copolymerization (1) with stannous octoat as an initiator:

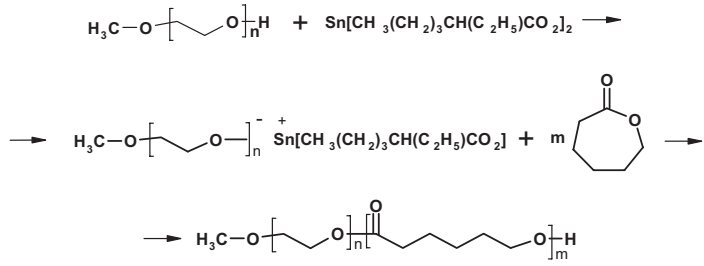

1

To 10 g of MOPEG well dried under vacuum, in an inert atmosphere a necessary quantity of ε-caprolactone, which was distilled exactly before a synthesis, and stannous octoat were added. The reaction of a block copolymerization was carried out at 135 °C for 24 h. Taking into account that stannous octoat acted as initiator,[22] but not as catalyst of the block copolymerization (as it was considered in some earlier publications[23,24]), the molar ratio $[Sn(Oct)_2]/[MOPEG] = 1$ was used in all the cases. Also, unlike the synthesis protocol by Bogdanov[21] and other researchers,[25] the resulted product was dissolved in dioxane and then, after methanol was added to complete the "living" copolymerization process and to remove stannous octoat from the chain ends, was precipitated by ethanol and dried in a vacuum case at 40 °C. Stannous octoat wasn't able to initiate the homopolymerization of ε-caprolactone in the reaction blend in the absence of low-molecular-weight alcohols.[26,27] Thus, the reaction product could not contain PCL homopolymer. Possible admixture of pure MOPEG was separated by dissolution and re-precipitation of the final product. To define a chemical structure and molecular weights of the copolymers, FTIR and ^{1}H nuclear magnetic resonance (NMR) spectroscopy were used.

FTIR spectra of MOPEO-*b*-PCL and initial MOPEG were recorded in diluted solutions ($C = 2.5$ kg · m^{-3}) in an inert solvent CCl_4 by a "Nexus-470 Nicolet" spectrometer (USA) with a resolution 4 cm^{-1}. Polymer solutions were placed in a collapsible cylindrical cavity, made from sodium chloride, with the thickness of $l = 0.6$ mm. Also FTIR spectroscopy was used to define the nature of DBC interaction with a model drug PS. In this case FTIR spectra were recorded for one of DBC samples, PS and DBC + PS blend in potassium bromide medium and/or in the form of a thin film, cast on fluorite glasses. All the spectra were recalculated in the dependences of the optical density (D) versus the wavenumber (ν) using the relation: $D = \lg T_0/T$, where T_0 and T are maximum and current values of the transmission.

^{1}H NMR spectra of DBCs and MOPEG were recorded in CCl_4 at 20 °C and $C = 10$ kg · m^{-3} by a 400 MHz "Mercury-400" spectrometer from "Varian" (USA). The relative integral intensities of the proton signals were calculated using NUTS program.

To investigate a bulk structure of initial MOPEG and DBCs the methods of differential scanning calorimetry (DSC) and wide-angle X-ray scattering (WAXS) were used. A differential microcalorimeter DSC-910 and thermoanalizer 1090 from "Du Pont" (USA) were applied in DSC method. Every sample (~10 mg) was introduced into the open DSC pan and heated from −150 to 200 °C with a rate of 16 K · min^{-1} (the 1-st scan). Then it was sharply cooled with liquid nitrogen up to an initial temperature and heated again with the same rate (the 2-nd scan). The instrument was calibrated with indium and zinc to determine thermodynamic parameters of structural transitions. Also, a sapphire crystal with $m = 61.66$ mg was heated with (co)polymer samples to obtain the dependences of the specific heat capacity (C_p) versus the temperature. WAXS profiles of initial MOPEG and DBCs were obtained using a DRON-2.0 X-ray difractometer. The (co)polymer samples were dried in a vacuum desiccator for one week. The samples with a thickness of ~1 mm were used for the measurements. The monochromatic Cu-K_α radiation with $\lambda = 0.154$ nm, filtered by Ni, was provided by an IRIS-M7 generator at an operating voltage of 30 kV and current of 30 mA. The scattering intensities were measured by a scintillation detector scanning in 0.2° steps over the range of the $\theta = 3 - 40$° scattering angles. The obtained diffraction curves were reduced to equal intensities of the primary beam and equal values of the scattering volume.[28] Also, the normalization of experimental scattering intensities was carried out according to the formula:

$$I_{n(i)}(\theta) = [I_{\exp}(\theta) - I_b(\theta)] \cdot (I/I_0),$$

were $I_{exp}(\theta)$ and $I_{n(i)}(\theta)$ are the experimental and normalized intensities in WAXS profile as a function of θ, $I_b(\theta)$ is the intensity of

the background for every θ value, I_0 and I are the intensities of incident and scattered beams at $\theta = 0^\circ$ (the coefficient of the beam weakening).

The micelle formation of DBCs and those in the presence of the drug in dioxane/aqueous solutions was studied using visible spectroscopy. The optical density of all the solutions was measured at a room temperature and $\lambda = 500$ nm with UV/VIS spectrometer ''Perkin Elmer Lambda 20'' (Sweden). To determine the critical micellization concentrations (*CMC*s) of these systems by static light scattering (SLS), a modernized instrument ''FPS-3'' (Russia), equipped with a light-emitting diode WP7113VGC/A from ''Kingbright'', the controller ADC-CPU^{TM} from ''Insoftus'' (Ukraine) and the computer program ''WINRECORDER'', was applied. The scattering intensities (I_v) of the vertically polarized incident light with $\lambda = 520$ nm were determined at the scattering angle $\theta = 90^\circ$ in a vide region of the diblock copolymer concentrations. All solutions were prepared using dust-free deionized water and dust-free dioxane, and kept in a special dust-free box for 24 h to achieve a thermodynamic equilibrium.

Chemical Structure and Molecular Parameters

Chemical structure of synthesized DBCs was confirmed firstly by FTIR (Figure 1). In MOPEG spectrum split bands of ν_{COCas} and ν_{COCs} vibrations with medium intensity (at 1217 cm^{-1}, 1252 cm^{-1} and 978 cm^{-1}, 1005 cm^{-1} correspondingly) and also the less intensive vibration bands of $\nu_{COCH3as}$ and ν_{COCH3s} (at 1110 cm^{-1} and 1068 cm^{-1}) were displayed (Figure 1a, spectrum *1*). In DBC2 spectrum (Figure 1a, spectrum *2*) the intensity of the band at 1217 cm^{-1} changed and a new vibration band at 1163 cm^{-1} appeared that indicate the appearance of $\nu_{COC(O)as}$ and $\nu_{COC(O)s}$ vibration bands of PCL blocks.[22]

Also, in DBC2 spectrum ν_{CO} vibration band of a medium intensity at 1737 cm^{-1}, which is characteristic for PCL ester groups,[29] was observed. In this region of MOPEG and DBC spectra an intensive ν_{CCl} vibration band, which belonged to the solvent (CCl_4), was displayed too. The spectrum of MOPEG in the region of 2400–4000 cm^{-1} (Figure 1b, spectrum *1*) demonstrated two ν_{CH} vibration bands of methyl and methylene groups at 2871 cm^{-1} and 2920 cm^{-1}, which were strongly overlapped. At the same time, DBC spectrum (Figure 1b, spectrum *2*) showed an intense band at 2944 cm^{-1}, which corresponded to ν_{CH} vibrations of the PCL central methylene groups, that was an additional confirmation of MOPEO and PCL presence in the copolymers.

A chemical nature and the main molecular parameters of DBCs were characterized also by ^{1}H NMR spectroscopy; the examples are shown in Figure 2.

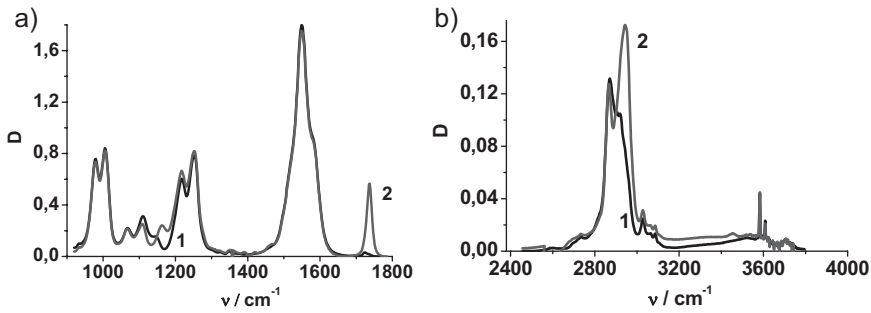

Figure 1.
The example of FTIR spectra, recorded in CCl_4, in the regions of (**a**) ν_{COC}, $\nu_{COC(O)}$, ν_{CO} vibrations and (**b**) ν_{CH}, ν_{NH}, ν_{OH} vibrations for: MOPEG –*1* and DBC2–*2*; $T = 20\,^\circ$C.

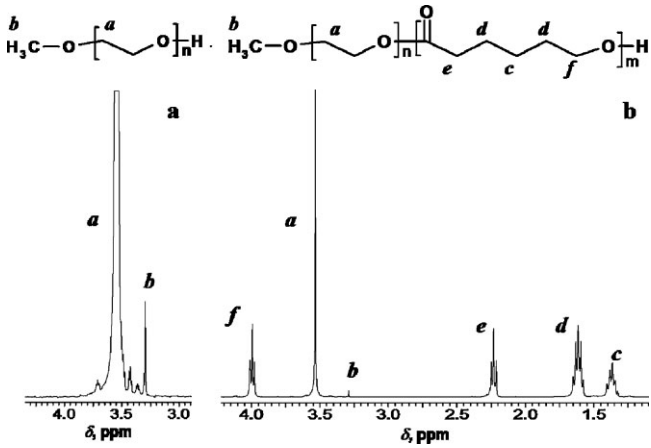

Figure 2.
^{1}H NMR spectra of (**a**) MOPEG and (**b**) DBC2 in CCl_4; $T = 20\,^{\circ}C$.

In MOPEG spectrum two resonance signals with the chemical shifts $\delta = 3.54$ and 3.30 ppm (Figure 2a), which could be attributed to the protons of methylene (***a***) and terminal methoxy (***b***) groups, were present. In the spectrum of DBC2 (Figure 2b) four groups of signals with $\delta_{max} = 1.37,\ 1.62,\ 2.24$ and 4.00 ppm were additionally displayed. They corresponded to the protons of a central methylene group (***c***) in PCL unit, two methylene groups near the central one (***d***), one methylene group near carbonyl (***e***), and one methylene group, disposed near oxygen atom of ester group (***f***), consequently. The interpretation of spectra was carried out in accordance with the data of the atlas[29] and other studies.[30] Using the following formulas, the number average molecular weights of MOPEG (M_{nMOPEG}) and PCL (M_{nPCL}) blocks in DBCs were calculated (Table 1):

$$M_{nMOPEG} = \frac{3 \cdot M_{0MOPEG} \cdot A_a}{4 \cdot A_b};$$

$$M_{nPCL} = \frac{M_{0PCL} \cdot M_{nMOPEG} \cdot A_d}{M_{0MOPEG} \cdot A_a},$$

where $M_{0\ \mathrm{MOPEG}}$ and $M_{0\ \mathrm{PCL}}$ are the molecular weights of MOPEG and PCL units. These relations are based on the integral intensities (A) of the signals ***a*** and ***b*** (in the case of MOPEO blocks) and ***a*** and ***d*** (in the case of PCL blocks). The molecular weights of DBCs were found as sum: $M_{n\mathrm{DBC}} = M_{n\mathrm{MOPEO}} + M_{n\mathrm{PCL}}$.

Table 1.
The main molecular parameters of obtained series MOPEO-*b*-PCL copolymers

Copolymer	$M_{n\mathrm{MOPEO}}$ kDa	$M_{n\mathrm{PCL}}$ kDa	$M_{n\mathrm{DBC}}$ kDa	$n^{a)}$
DBC1	2.5	2.8	5.3	0.42
DBC2	2.5	8.0	10.5	1.25
DBC3	2.5	23.9	24.6	3.68
DBC4	2.5	24.3	26.8	3.74

[a)]The ratio between PCL and MOPEO units in DBC.

It is seen that the length of hydrophobic PCL block in DBCs varies, while the hydrophilic MOPEO block retains the constant length. Indeed, in DBC1 sample PCL block turned out to be in 2.4 times shorter than MOPEO block. The second DBC2 sample was composed of the blocks with approximately equal length, but the next DBC3 and DBC4 copolymers contained PCL chains, which length was more than in 3 times higher than that of MOPEO block. Thus, a series of the diblock copolymers with different length of hydrophobic blocks was obtained.

Bulk Structure

Structural researchers of DBCs were of special interest because of the ability to

crystallization of both the blocks. Moreover, the temperatures of their glass and melting transitions is known to be close.[31] In spite of studies, which were devoted to a crystalline state or crystallization of covalently bound PCL and (MO)PEO chains in block copolymers,[32,33] we also carried out some structural investigations of the synthesized DBC samples using DSC and WAXS (Figure 3).

Traditionally, the only melting peak (at 53 °C) was displayed in DSC thermogram

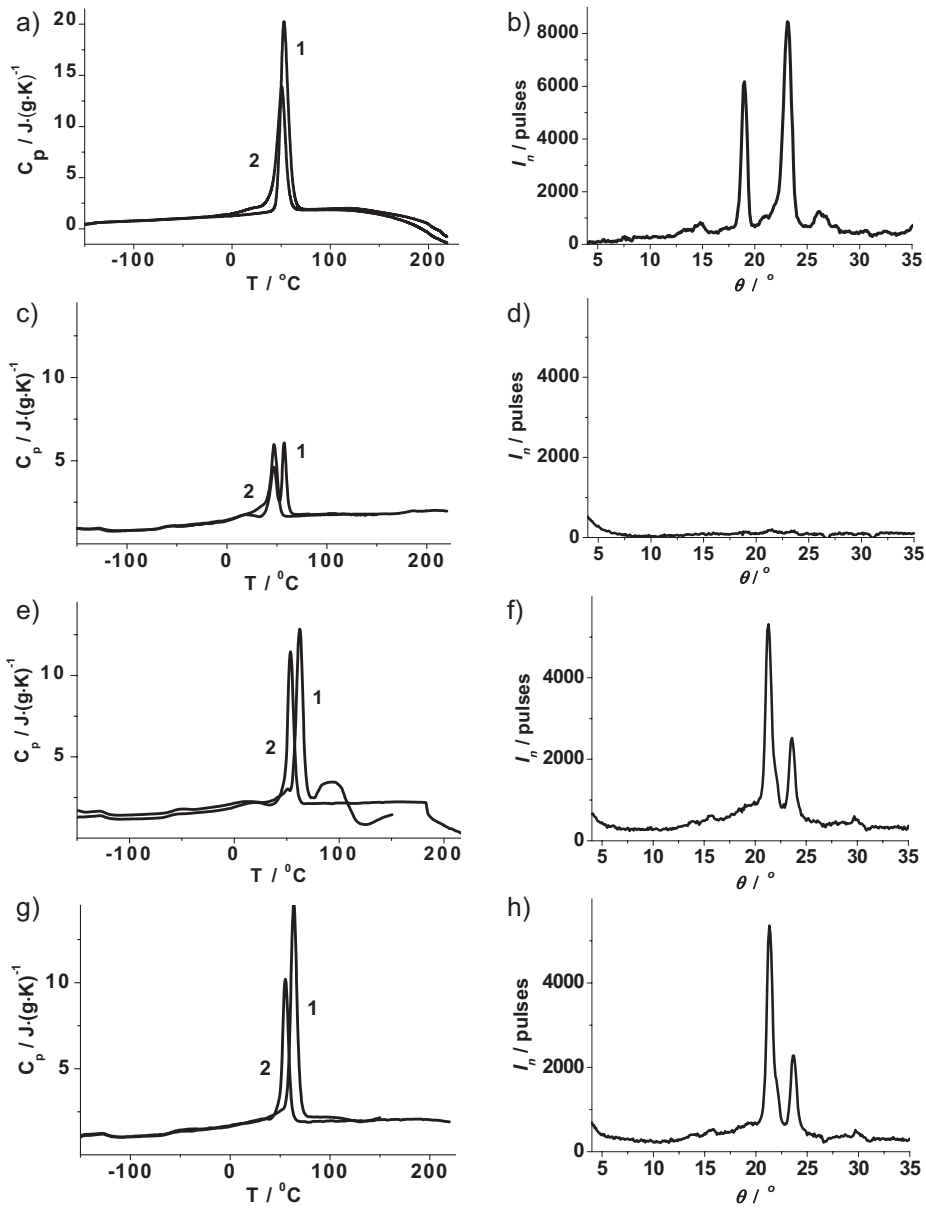

Figure 3.
(**a**, **c**, **e**, **g**) DSC thermograms (the first –1 and the second –2 scans) and (**b**, **d**, **f**, **h**) WAXS profiles for: (**a**, **b**) MOPEG, (**c**, **d**) DBC1, (**e**, **f**) DBC2 and (**g**, **h**) DBC3.

Table 2.
Parameters of thermal transitions in MOPEG and DBC bulk structure

Polymer	T_g [a] °C	ΔT_g [b] °C	Δc_p [c] J · (g · °C)$^{-1}$	Melting peaks	T_m [d] °C	ΔT_m [b] °C	ΔH_m [e] J · g^{-1}	X_c [f] %
MOPEG	–		–	–	53.0	39	194.8	99.0
DBC1				1	19.5	34	4.8	–
	−63.5	13	0.20	2	47.0	19	22.7	24.4
				3	57.4	21	23.3	32.2
DBC2				1	14.0	34	2.4	–
	−58.5	13	0.28	2	51.0	40	6.4	13.7
				3	62.5	23	80.7	76.9
DBC3				1	14.2	27	0.7	–
	−57.0	18	0.30	2	~51	~25	~2.9	~15.5
				3	64.0	27	103.8	83.4
DBC4				1	19.4	25	0.6	–
	−58.0	12	0.29	2	~51	~23	~2.5	~13.7
				3	64.5	31	94.8	76.0

[a]The glass transition temperature.[b]The temperature range for a certain thermal transition.[c]The specific capacity jump.[d]The melting temperature.[e]The melting enthalpy.[f]The crystallinity degree: for MOPEG $X_c = \Delta H_m/\Delta H^\circ_m$, where ΔH°_m is the melting enthalpy for 100% crystalline PEO (196.8 J · g^{-1})[34], but for MOPEO and PCL blocks in DBC $X_c = \Delta H_m/(\Delta H^\circ_m \cdot w)$[34], where w is the weight fraction of the blocks in DBC; $\Delta H^\circ_m = 137.5$ J · g^{-1} for 100% crystalline PCL.[32]

of MOPEG (Figure 3a), while the glass transition did not observe because of its high crystallinity (Table 2). Unlike this, DSC thermograms of all the copolymers (the data for DBC4 were analogous to those for DBC3, so they are not presented) showed as one glass transition as 3 melting peaks (Figure 3c, e, g). Some melting peaks in DSC thermograms were strongly overlapped; therefore, an ordinary computer program of the instrument allowed determining only approximate parameters of them (Table 2). In our analysis we used the parameters, obtained only from the 1-st scan, because the processes of DBC and MOPEG crystallization under sharp cooling of the samples (~300 °C · min^{-1}) before the 2-nd scan were essentially non-equilibrium.

The thermal transition parameters in Table 2 (obtained from the 1-st scans) should be discussed with regard to the dependence on the PCL block length. According to the data of the study[32] and the changes in the intensity of melting peaks (ΔH_m in Table 2) with DBC content, the 2-nd peak with $T_m \sim 47 \div 51$ °C could be attributed to the melting of PEO microcrystalline domains. The 3-rd most intense peak with $T_m = 57.4 \div 64.5$ °C reflects to the melting process in separate microcrystalline regions of PCL. The nature of the 1-st melting peak in the range of $T_m = 14.0 \div 19.5$ °C is not clear yet. But it had too small intensity (Table 2) and was not taken into consideration.

T_m values for the PCL microcrystalline regions grew up to the constant value at the increase in PCL length (and the weight fraction). It was accompanied by an essential enhance in the crystallinity degree (X_c) of these blocks. The last parameter achieved the maximum value 83.4% in the case of DBC3 and then (for DBC4) it some reduced. In parallel, X_c value for MOPEO block decreased (Table 2). Interestingly, X_c value for MOPEO blocks turned out to be less than that for PCL blocks even in the case of DBC1, which polyether block was significantly longer than polyester one. Taking into account higher crystallization rate of PCL chains compared to PEO[32], the conclusion about a depression of the MOPEO block crystallization due to a primary crystallization of PCL blocks could be achieved. The glass transition parameters changed in full accordance with these data. Really, T_g value for a pure PCL (near −59 °C)[34] is some higher than that for a pure PEO (−57 °C)[35]. Therefore,

when the relative length (the weight part) of PCL blocks and their crystallinity degree in DBC structure grew, the fraction of PCL segments in amorphous regions decreased and T_g number reduced up to the value, which is characteristic for a pure PEO (Table 2).

The data of WAXS was in a full accordance with the described data of DSC. Actually, highly crystalline structure of MOPEG was reflected in WAXS profile by two intense crystalline peaks at the scattering angles $\theta = 19.0^\circ$ and 23.1° (Figure 3b), which are well known from the literature.[34] Low X_c values for MOPEO blocks in the structures of DBC2-DBC4 samples (Table 2) fully correlate with practical disappearance of both peaks in corresponding WAXS difractograms (Figure 3f, h). Instead of them, in these profiles two other crystalline peaks at $\theta = 21.3^\circ$ and 23.6°, which are characteristic for the crystalline regions of a pure PCL,[33,34] could be observed. Finally, both groups of peaks were practically absent (had too small intensity) in the difractogram of DBC1 sample contained the shortest PCL block (Figure 3d). This fact was in full agreement with low enough X_c numbers for both the blocks in DBC1 structure (Table 2). A mutual negative influence of covalently bound blocks on the processes of their crystallization was clearly displayed in this case.

Using well-known Bregg's relation: $d = \lambda/[2 \cdot \sin(\theta/2)]$,[28] we have calculated the average interplane distances in crystalline lattice of MOPEG and DBCs; they are shown in Table 3.

Table 3.
Characteristics of crystalline lattice according to WAXS profiles

Polymer	The maximum positions		The average interplane distances	
	θ_1 degrees	θ_2 degrees	d_1 nm	d_2 nm
MOPEG	19.0	23.1	0.467	0.385
DBC1-DBC4	21.3	23.6	0.416	0.377

Micellization in the Mixed Solvent

Dioxane was a good solvent for the whole MOPEO-*b*-PCL chains, while water was able to dissolve selectively only MOPEO blocks. Taking into account these facts, we initiated self-assembly of DBC macromolecules by a sequence addition of water in dioxane solutions of the copolymers. In order to characterize the micellization process, the optical density (turbidity) of the DBC dioxane/aqueous solutions with constant $C_{DBC} = 0.8\,\mathrm{kg \cdot m^{-3}}$ was measured in the visible region of the spectrum at a different content of the selective solvent (Figure 4a).

Corresponding increase in the solution turbidity since approximately 20 v % of water was established. Moreover, an essential intensification of the micellization process took place at the lengthening of PCL blocks (Figure 4a, ▲ ●). To carry out detail investigations of the effect of the hydrophobic block length on thermodynamic parameters of the micellization process, a stable composition of the mixed solvent (dioxane/H_2O = 30/70 v/v, %) was chosen. The *CMC* and $-\Delta G^\circ$ values are important parameters for concerned systems because they characterize the size and stability of micelles, that is important for the prolonged circulation of the micellar therapeutic systems in the bloodstream without any degradation and the risk to be captured by the macrophages from the reticuloendothelial system of organisms.[16] Also, *CMC* value correlates with the drug quantity, which could be incorporated in the micellar ''core''.

CMC values, found for DBC2-DBC4 samples by both Vis spectroscopy (Figure 4b) and SLS (Figure 4c), are compared in Table 4. It is evident that SLS is more sensitive method for such determinations and provides more exact and lower *CMC*s. The values of the Gibbs free micellization energy, which were calculated according to the known relation: $\Delta G^\circ \approx RT \cdot \ln CMC$, are also represented in Table 4. These data show a regular reduction in *CMCs* and increase in $-\Delta G^\circ$ numbers (as in the stability of DBC micelles) with growth of

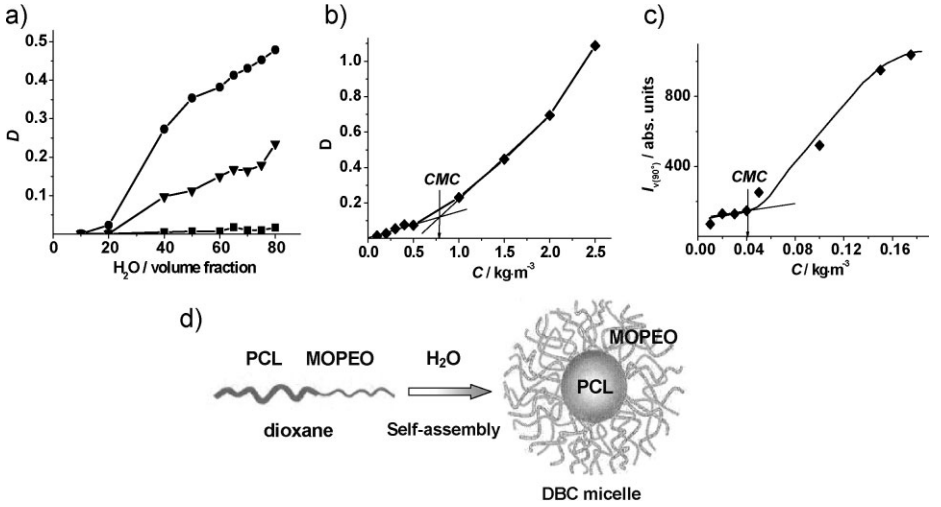

Figure 4.
(**a**) Dependences of the optical density (turbidity) of the diblock copolymer dioxane/aqueous solutions *vs* H_2O content; ■ = DBC1, ▲ = DBC2, ● = DBC3; the examples of *CMC* determinations for DBCs in the dioxane/H20 = 30/70 v/v, % solvent by (**b**) visible spectroscopy and (**c**) SLS; ◆ = DBC4, T = 20 °C; (**d**) a scheme of DBC micellization in the mixed solvent.

the hydrophobic block length. Such effects are typical for the majority of amphiphilic diblock copolymers.[14]

Micelle formation in DBC solutions at high water content could be represented by the following simplified scheme (Figure 4d). Here PCL blocks form a hydrophobic micellar ''core'', whilst MOPEO chains create a hydrophilic stabilizing ''corona''. At the lengthening of PCL block the relative size of ''core'' in spherical micelles would essentially grow. Due to this, corresponding changes in micellar morphology (transition from ''hairy-type'' micelles for DBC1 to ''crew-cut'' ones for DBC3 and DBC4) could be expected.

Table 4.
Parameters of the micellization process in DBC and DBC + PS solutions[a)]

System	$CMC \cdot 10^5$		$-\Delta G^o$	
	mol/dm^3		kJ/mol	
	Vis	SLS	Vis	SLS
DBC2	8.78	0.48	22.91	27.80
DBC3	3.69	0.08	25.04	31.87
DBC4	3.04	0.15	25.57	30.44
DBC2 + PS[b)]	6.93	–	23.56	–
DBC3 + PS	2.80	–	25.79	–
DBC4 + PS	1.87	–	26.79	–

[a)]Dioxane/H_2O = 30/70 v/v.[b)]The ratio of $\varphi = 0.25\ mol_{PS}$/base-mol_{DBC}.

Studying the effect of water-insoluble drug PS on DBC self-assembly in the same mixed solvent was of special interest. For these experiments the constant ratio between the drug and the copolymers ($\varphi = [PS]/[DBC] = 0.25\ mol_{PS}$/base-$mol_{DBC}$) was chosen. This ratio was corresponded to the complete drug binding by the micelles of polymer carrier, which was established by preliminary experiments. The data, obtained in this case by visible spectroscopy (Figure 5a, b, c), showed an exact reduction in *CMC* numbers (Table 3), caused by PS binding with the copolymer micelles.

Lower values of the optical density in DBC4 + PS system (Figure 5c) unlike two other ones (Figure 5a, b) could be explained by a very intensive micellization, that initiated some phase separation in the measuring cavity. *CMC* and $-\Delta G^\circ$ values for the DBC micellization processes turned out to be less and higher correspondingly, than those for analogous processes in the drug-free solutions (Table 4). It meant that prednisolon actively participated in

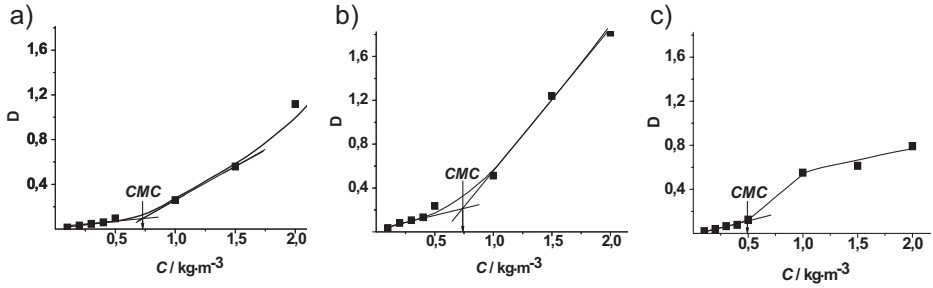

Figure 5.
Dependences of the optical density *vs* the copolymer concentration in (**a**) DBC2 + PS, (**b**) DBC3 + PS, and (**c**) DBC4 + PS dioxane/water (30/70 v/v) solutions; $\varphi = 0.25\ mol_{PS}/base\text{-}mol_{DBC}$, $T = 20\ ^{\circ}C$.

the micelle formation of DBCs and acted as an additional stabilization factor for DBC + PS micellar system that was evidently conditioned by the drug interaction with MOPEO-*b*-PCL micelles. Such block copolymer micelles with associated drug could be the basis for creation of biologically-functional nanoparticles. The micelle formation and the drug incorporation process could be performed in mixed solvent (dioxane/H_2O), and then prepared solutions of micelles, filled by drug, could be purified from dioxane by prolonged dialysis against water.[14]

The Drug Interaction with Copolymer Micelles

In the next part of our work we studied the nature of PS interaction with DBC micelles. Taking into account a chemical structure of the drug (2), included two carbonyl and three hydroxyl (primary, secondary and tertiary) groups, and potential ability in hydrogen bonding of PS hydroxyls with proton-acceptor groups of DBC macromolecules only, we applied FTIR spectroscopy in order to test the existence of such H-bonds.

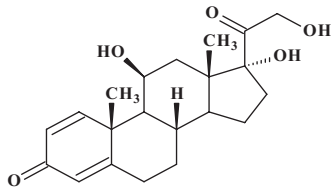

2

FTIR spectra of a commercial PS, one of DBC samples and their blend with $\varphi = 0.25\ mol_{PS}/base\text{-}mol_{DBC}$ in two most important regions are exhibited in Figure 6. All the spectra were interpreted in accordance to the literature data.[36,37]

The spectra of thin films of a pure DBC2 and DBC2 + PS blend are shown in Figure 6a, b (curves *1, 2*). Unlike this, the other spectra in Figure 6 corresponded to (c, d) the above substances and (e, f) pure PS in potassium bromide. In the spectra of DBC2 there were two intense overlapping bands of $\nu_{C=O}$ vibrations at $\sim 1735\ cm^{-1}$ and $1724\ cm^{-1}$ (in film) or $1726\ cm^{-1}$ (in potassium bromide) for PCL ester groups, which were located in the amorphous and crystalline regions, consequently (Figure 6a, c, curves *1*). In the other region of spectra (Figure 6b, d, curves *1*) the bands of $\nu_{C\text{-}H}$ vibrations of a hydrocarbon skeleton of both the blocks were observed. Moreover, DBC2 spectrum in potassium bromide (Figure 6d, curve *1*) demonstrated also a wide band of $\nu_{O\text{-}H}$ vibrations at $3437\ cm^{-1}$ for probably H-bonded terminal hydroxyl groups of PCL and/or some water molecules. Note, that this band was practically absent in the case of a carefully dried DBC2 thin film (Figure 6b, curve *1*).

The spectrum of the crystalline drug in potassium bromide (Figure 6e, f) contained the bands of $\nu_{C=O}$ vibrations at $1707\ cm^{-1}$ and $1657\ cm^{-1}$ for the free and H-bonded carbonyl groups, the bands of $\nu_{C=C.as}$ and $\nu_{C=C.s}$ vibrations at $1616\ cm^{-1}$ and $1602\ cm^{-1}$ for two unsaturated bonds in

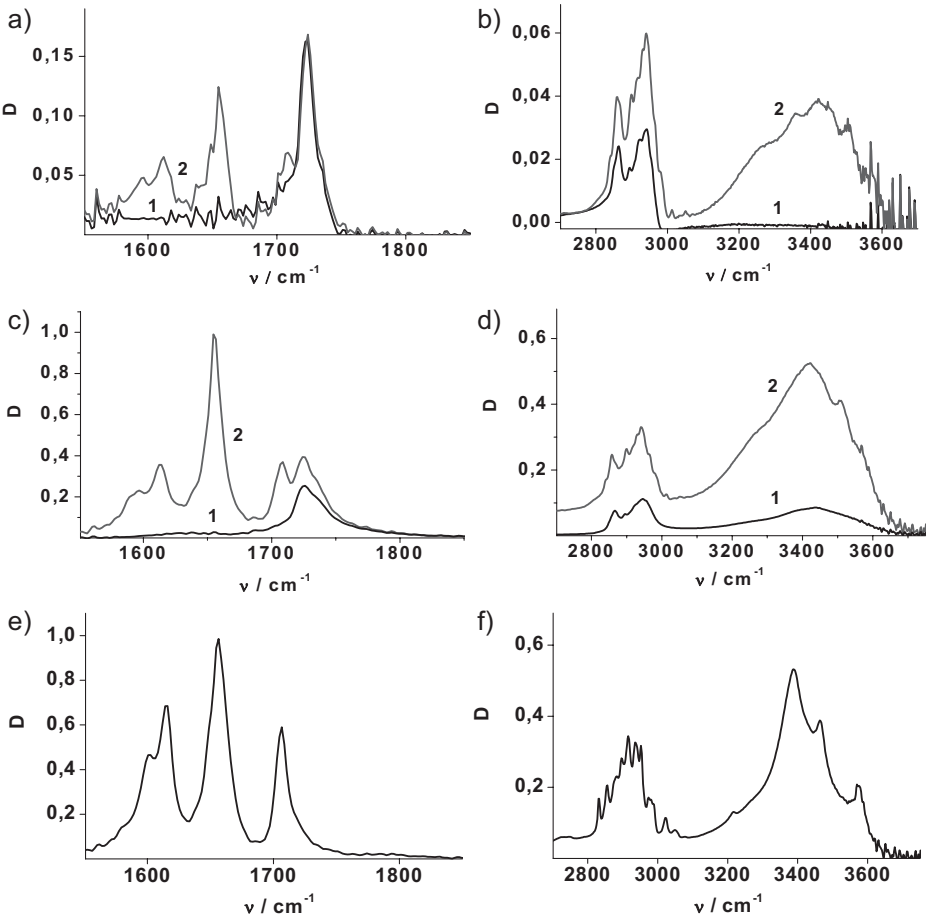

Figure 6.
FTIR spectra in the regions of (**a**, **c**, **e**) $\nu_{C=C}$, $\nu_{C=O}$ and (**b**, **d**, **f**) $\nu_{C\text{-}H}$, $\nu_{O\text{-}H}$ vibrations for DBC2–1 and DBC2 + PS –2 thin films ($l \sim 4$–$5\ \mu m$) cast on (**a**, **b**) fluorite glasses, for DBC2 and DBC2 + PS in (**c**, **d**) potassium bromide and also for commercial PS in (**e**, **f**) potassium bromide.

one of PS rings as well as the bands of $\nu_{O\text{-}H}$ vibrations at $3575\,cm^{-1}$, $3464\,cm^{-1}$ and $3388\,cm^{-1}$ for the H-bonded $-OH$ groups. It was evident that three different (in energy) H-bonds, which displayed in PS spectrum, stabilize its crystalline structure.

FTIR spectra of DBC2 + PS blend, which were recorded for a thin film (Figure 6a, b, curves *2*) and a pill with potassium bromide (Figure 6c, d, curves *2*), did not show noticeable alterations in the positions of $\nu_{C=O}$ and $\nu_{C=C}$ vibration bands (Figure 6a, c), thus did not confirm the existence of H-bonds between PS and DBC. It was connected with the strong overlapping of the above-considered bands of both components. At the same time, in the region of $\nu_{O\text{-}H}$ vibrations (Figure 6b, d) two important effects could be marked. The first one consisted in a significant (on $33\,cm^{-1}$ and $40\,cm^{-1}$) high-frequency shift of $\nu_{O\text{-}H}$ vibration bands of PS (at $3388\,cm^{-1}$ and $3464\,cm^{-1}$, consequently) and a small (on $7\,cm^{-1}$) low-frequency shift of the third analogous PS band (at $3575\,cm^{-1}$). These facts indicated the partial destruction of the initial hydrogen bond system in PS crystals under the effect of DBC and could be considered as an indirect with the drug. But the second effect: an appearance of two

new $\nu_{O\text{-}H}$ vibration bands at 3284 cm^{-1} and 3358 cm^{-1}, brightly displayed in the spectrum of thin film (Figure 6b, curve *2*), allowed us to make the final conclusion about hydrogen bonding of PS with DBC.

The proton-accepting capability of ether groups is known to be some higher than that of ester groups.[16,17] Thus, the drug molecules would be previously concentrate in the micellar ''corona'', formed by MOPEO blocks. Moreover, the developed hydrophobic parts of PS molecules would be promoted to their penetration into the ''core'' of micelles with PCL blocks, thus ensuring an additional stabilization for whole micellar system.

Conclusion

Biocompatible and biodegradable amphiphilic diblock copolymers MOPEO-*b*-PCL with the constant length of MOPEO blocks ($M_n = 2.5$ kDa) and varied length of PCL blocks ($M_n = 2.8 \div 24.3$ kDa) self-assembled in dioxane/aqueous solutions into the micelles with hydrophobic ''core'' of PCL blocks, and hydrophilic ''corona'' formed by MOPEO blocks. The micelle stability regularly grew with increase in the length of PCL blocks that appeared in the lowering *CMC* values and enhance in $-\Delta G^{\circ}$ numbers. The micelles actively connected with the model drug prednisolon by means of hydrogen bonds between ether or ester groups of the copolymer and hydroxyl groups of the drug and also by hydrophobic interactions. This accompanied by the increase in stability of micellar particles. Thus, MOPEO-*b*-PCL micelles could be considered as perspective delivery systems, which stability would only grow at the encapsulation of many toxic and poorly soluble drugs. Moreover, an additional increase in stability of these micelles filled by drugs could be expected at the following preparation of the ready-for-use nanoparticles (''frozen'' micelles[14]) by the dialysis of dioxane/aqueous micellar solutions against water.

The structural investigations of DBCs revealed the existence of amorphous regions and microcrystalline domains, formed by both PCL and MOPEO blocks separately, and displayed a mutual negative influence of covalently bound blocks on the processes of their crystallization.

[1] C. Kaparissides, S. Alexandridou, K. Kotti, S. Chaitidou, *J. Nanotechnology Online* **2006**, *2*, 1.
[2] Y. Takakura, M. Hashida, *Pharmaceutical Reserch* **1996**, *13*(6), 820.
[3] Z. M. Qian, H. Li, H. Sun, K. Ho, *Pharmacol. Rev.* **2002**, *54*(4), 561.
[4] S. A. Wissing, O. Kayser, R. H. Müller, *Advanced Drug Delivery Reviews* **2004**, *56*, 1257.
[5] W. Ulbrich, A. Lamprecht, *J. R. Soc. Interface* **2010**, *7*, s55.
[6] K. Cho, X. Wang, S. Nie, Z. Chen, D. M. Shin, *Clin. Cancer Res.* **2008**, *14*(5), 1310.
[7] S. Gelperina, K. Kisich, M. D. Iseman, L. Heifets, *Am. J. Respir. Crit. Care Med.* **2005**, *172*, 1487.
[8] T. C. Yih, M. Al-Fandi, *J. Cel. Biochem.* **2006**, *97*, 1184.
[9] P. W. Taylor, C. Howes, *Biotherapy* **1991**, *3*, 1.
[10] C. Allen, Y. Yu, D. Maysinger, A. Eisenberg, *Bioconjugate Chem.* **1998**, *9*, 564.
[11] C. Allen, J. Han, Y. Yu, D. Maysinger, A. Eisenberg, *J. Controlled Release* **2000**, *63*, 275.
[12] D. K. Kim, J. Dobson, *J. Mater. Chem.* **2009**, *19*, 6294.
[13] G. Orive, R. M. Hernández, A. R. Garcón, J. L. Pedraz, *Cancer Therapy* **2005**, *3*, 131.
[14] G. Riess, *Prog. Polym. Sci.* **2003**, *28*, 1107.
[15] C. Allen, A. Eisenberg, D. Maysinger, *S. T. P. Pharma Sci.* **1999**, *9*, 139.
[16] J. Lee, H. Lee, J. Andrade, *Prog. Polym. Sci.* **1995**, *20*, 1043.
[17] R. Savic, L. Luo, A. Eisenberg, D. Maysinger, *Science* **2003**, *300*, 615.
[18] L. Luo, J. Tam, D. Maysinger, A. Eisenberg, *Bioconjugate Chem.* **2002**, *13*, 1259.
[19] P. Ghoroghchian, G. Li, D. Levin, K. Davis, F. Bates, D. Hammer, M. Therien, *Macromolecules* **2006**, *39*, 1673.
[20] L. Bromberg, E. Magner, *Langmuir* **1999**, *15*, 6792.
[21] B. Bogdanov, A. Vidts, A. V. D. Bulcke, R. Verbeeck, E. Schacht, *Polymer* **1998**, *39*, 1631.
[22] T. Zheltonozhskaya, S. Fedorchuk, V. Syromyatnikov, *Russ. Chem. Rev.* **2007**, *76*, 731.
[23] M. Yuan, Y. Wang, X. Li, C. Xiong, X. Deng, *Macromolecules* **2000**, *33*, 1613.
[24] H. M. Aliabadi, A. Mahmud, A. D. Sharifabadi, A. Lavasanifar, *J. Controlled Release* **2005**, *104*, 301.
[25] P. L. Soo, L. Luo, D. Maysinger, A. Eisenberg, *Langmuir* **2002**, *18*, 9996.
[26] H. R. Kricheldorf, S. Rost, Ch. Wutz, A. Domb, *Macromolecules* **2005**, *38*(16), 7018.
[27] M. Huang, S. Li, M. Vert, *Polymer* **2004**, *45*, 8675.

[28] Yu. S. Lipatov, V. V. Shilov, Yu. P. Gomza, et al., X-Ray Diffraction Methods to Study Polymeric Systems, Nauk. Dumka, Kyiv **1982**, [in Russian].
[29] E. Pretsch, P. Bullman, C. Affolter, Structure determination of organic compounds. Tables of spectral data "Mir", Moskva, **2006**.
[30] F. Meng, S. Zheng, T. Liu, *Polymer*. **2006**, *47*, 7590.
[31] H. Takeshita, K. Fukumoto, T. Ohnishi, T. Ohkubo, M. Miya, K. Takenaka, T. Shiomi, *Polymer* **2006**, *47*, 8210.
[32] Y. Zhao, X. Fan, X. Chen, X. Wan, Q. Zhou, *Polymer* **2005**, *46*, 5396.
[33] A. Farah, N. Hall, S. Morin, W. Pietro, *Polymer* **2006**, *47*, 4282.
[34] C. Wu, *Polymer* **2005**, *46*, 147.
[35] S. V. Fedorchuk, T. B. Zheltonozhskaya, N. M. Permyakova, Y. P. Gomza, S. D. Nessin, V. V. Klepko, *Molecular Cryst. Liquid Cryst.* **2008**, *497*, 268.
[36] L. Bellamy, R. Pace, *Spectrochimica Acta*. **1969**, *25A*, 319.
[37] J. Dechant, R. Danz, W. Kimmer, R. Schmolke, Infra-red spectroscopy of polymers, "Khimiya", Moskva, **1976**.

